Article

Encapsulation of Inorganic Nanoparticles by Anionic Emulsion Polymerization of Diethyl Methylene Malonate for Developing Hybrid Microparticles with Tailorable Composition

Shreyas Joshi [1], John Klier [2] and Peter J. Beltramo [1,*]

[1] Department of Chemical Engineering, University of Massachusetts Amherst, Amherst, MA 01003, USA
[2] School of Chemical, Biological and Materials Engineering, University of Oklahoma, Norman, OK 73019, USA
*   Correspondence: pbeltramo@umass.edu

Abstract: Colloidal particle self-assembly into higher-ordered structures has been of great interest due to the promise of creating metamaterials with novel macroscopic properties. The physicochemical properties of these metamaterials can be tailored to achieve composites with tunable functionalities, either by controlling the assembly morphology and/or chemistry of the colloidal building blocks. This work describes a strategy of developing microparticles with a hybrid configuration that have an inorganic and an organic part. The inorganic part comprises functional nanoparticles, which are embedded within an organic polymer particle composed of diethyl methylene malonate polymer [p(DEMM)] prepared using anionic emulsion polymerization. DEMM polymerization is initiated entirely by the presence of hydroxyl anions and the resulting particle diameter can be tuned between 300 nm and 1 micrometer by reaction pH. Inorganic nanoparticles with varying chemistry (TiO$_2$, CdTe, ZnO) can be loaded into the p(DEMM) particle with a controlled weight fraction, as confirmed by thermogravimetric analysis. The colloidal stability of the composite microparticles is seen to be dependent on the ligand coating attached to the inorganic constituent. These results provide a synthetic groundwork for creating hybrid, stimuli-responsive microparticles.

Keywords: organic–inorganic microparticles; hybrid colloids; anionic emulsion polymerization; polymer colloids

1. Introduction

The self-assembly of both isotropic and anisotropic colloidal particles into complex structures has drawn significant attention due to the potential to engineer metamaterials with novel macroscopic properties [1–3]. The physicochemical properties of these metamaterials can be tailored to achieve composites with tunable functionalities. In particular, nanoscale inorganic constituents that have favorable properties for applications can be incorporated into a microscale organic polymer component to result in a composite system with enhanced macroscopic functionality [4,5]. To enable this technology, it is necessary to design a synthesis scheme that produces micron-sized composite particles with tunable properties.

The strategy of developing composite systems with functional constituents has already shown promise in a range of applications. For instance, inorganic nanoparticles (such as silica, gold, or iron oxide) coupled with polymers (poly(N-isopropylacrylamide-co-acrylamide), poly(2-vinylpyridine, poly-b-cyclodextrin)) creates multifunctional drug delivery systems whose components can orthogonally load drug molecules and release them via controlled stimuli response [6]. Titania (TiO$_2$) nanospheres have photocatalyst properties and are used to enhance the hydroxyl (OH-) radical generation by ultrasound irradiation, which can have applications in sonodynamic therapy [7,8]. Antimony-based hybrid organic–inorganic materials enhance the efficiency and stability of polymer solar cells [9]. A novel method for coating diethyl-5-hydroxyisophthalate (DEIP) as an organic

coating on ZrO_2, SiO_2, and TiO_2 nanoparticles using electron transfer technique gives self-cleaning and anti-corrosive properties to the metallic surfaces [10]. Monolayers of porous silica nanoparticles have been chemically etched on a polymer substrate for developing coatings with antireflective functionality [11–14]. Similar hybrid organic–inorganic configurations can be used effectively to construct systems with tunable functionalities that can then be transformed into coatings by sol-gel or lithographic techniques.

TiO_2 nanoparticles are of particular interest in the development of optically high impedance coatings due to their high refractive index [12,15–22]. Janssen et al. encapsulated TiO_2 nanoparticles using styrene and acrylate-based monomers and summarized the influence of process variables on the particle formation. The solvent polarity, surfactant concentration, monomer addition rate, and surface functionalization on the inorganic pigment was reported to affect the degree of encapsulation of inorganic constituents [23]. The degree of polymer encapsulation of the inorganic particles is difficult to control due to the individual and synergistic effects of various reaction parameters. The interaction of titania with styrene and acrylate monomers using free-radical emulsion polymerization resulted in a 70% polymer conversion and 20% encapsulation efficiency. Electrostatic interactions between the surface charge of the inorganic powder and the charge of the polymer chain end were seen to be critical for the reaction, with oppositely charged inorganic nanoparticles and polymer chain ends resulting in improved encapsulated microparticle yield [15]. In the case where calcium carbonate microparticles were encapsulated by methyl methacrylate (MMA) monomer using a similar polymerization mechanism, an increase in polymer content of the composite particles was reported. A preceding synthetic step of forming a primer layer of di(ethylene glycol) diacrylate (DEGDA) and MMA promoted the subsequent engulfment of the inorganic pigment by MMA. The DEDGA/MMA mixture was used to control the wetting of the calcite surface. The two-step encapsulation resulted in an encapsulation efficiency of 100% [24]. However, the encapsulated particles coagulated after formation, which is evident in the microscopy images.

The organic constituent of the synthetic scheme reported in this paper, diethyl methylene malonate (DEMM), is a novel monomer extensively studied by Huang et al. [25]. Two ester groups on the molecule allow the delocalization of negative charge, resulting in electropositivity and high reactivity of the vinyl groups on the molecule. This enables the anionic polymerization of DEMM to proceed in environmentally friendly conditions (room temperature and pressure). Huang et al. conducted anionic polymerization experiments with DEMM with varying pH [25]. The molecular weight of the polymerized DEMM was reported to increase with increasing pH, with a significant difference between pH 3–5 (MW < 32 kDa) and pH 6–7 (MW > 300 kDa). This was attributed to termination of the reaction by hydrogen ions (H+) dominating at low pH, whereas initiation by anionic hydroxyl groups (OH−) at high pH increased the rate of chain propagation, leading to low- and high-MW DEMM polymer being produced, respectively.

The present work describes a synthesis method for the formation of microparticles of hybrid inorganic–organic microstructure for achieving tailorable functional coatings. Our synthetic scheme is a simple method for encapsulating titania (TiO_2) nanoparticles within DEMM polymer microparticles using anionic polymerization. We extend the synthetic procedure to different inorganic constituents such cadmium telluride (CdTe) quantum dots and zinc oxide (ZnO) nanospheres for developing composite microparticles with unique functionalities. Several variables such as surfactant concentration, pH, monomer concentration and inorganic particle concentration are shown to influence the final hybrid particle characteristics.

2. Materials and Methods

2.1. Materials

DEMM (Chemilian M1000) was provided by Sirrus Inc. (Loveland, OH, USA) and used as received. Anionic surfactant sodium dodecyl sulfate (SDS) and hydrochloric acid (HCl) were used as received (Fisher Scientific, Hampton, NH, USA). Unfunctionalized titania nanoparticles (US Research Nanomaterials, Houston, TX, USA) with 30 nm diameter are initially used as the inorganic constituent in the synthesis scheme for developing hybrid inorganic–organic microparticles. The results from these experiments are then applied to other inorganic constituents such as pA-TiO$_2$ (TiO$_2$ which has been surface-functionalized with polyacrylic acid), CdTe quantum dots, and ZnO nanoparticles. The CdTe quantum dots are 10 nm in diameter and are surface-modified with 3 mercaptopropionic acid (3-MPA), an organosulfur compound that is a bifunctional molecule containing both carboxylic acid and thiol groups. The zinc oxide nanospheres (6 nm diameter) are capped with l-arginine ligand to induce a higher surface charge for better colloidal stability. Ultrapure deionized water (resistivity > 18.2 MΩ-com, MilliporeSigma, Burlington, MA, USA) was used in all cases.

2.2. Synthetic Scheme

We modify the anionic polymerization of DEMM by adding an inorganic pigment before initiating the polymerization to create polymer microparticles with embedded inorganic nanoparticles. First, inorganic nanoparticles were suspended in 10 mL deionized water at a concentration of 1 wt% in the reaction vessel. After several minutes of stirring, SDS was added to the solution to a final concentration of 6–9 mM. The surfactant acts as a colloidal stabilizer by inducing charge at the particle surface. A stronger charge leads to preferential monomer polymerization at the surface sites. Preliminary experiments found that hybrid particles that are synthesized at surfactant concentration higher than the CMC value result in larger globular particles; therefore, SDS concentrations at or below CMC were chosen for detailed study.

Next, the pH was adjusted to perform the synthesis at either acidic (4.5) or neutral (7.2) conditions by modifying the pH using 1 M HCl. Finally, after the pH adjustment, we introduced DEMM at a starved feeding rate of 1 mL/h. The polymerization of DEMM was initiated with an anionic hydroxyl group present in water or on the particle surface [25], allowing for control of the structure and composition of the resulting polymeric chains. The relatively slow rate of addition minimizes the secondary nucleation of the monomer in the solution [23]. The reaction was run for 4 h at room temperature with constant stirring at 600 rpm. To rapidly screen the experimental conditions outlined in the experimental design discussed in the next section, the synthesis was stopped by ending stirring, removing the supernatant of the reaction vial from the sedimented microparticles, and resuspending the particles in the same amount of reaction solvent. This sedimentation–resuspension procedure was performed 3 times before diluting 100 µL of particle solution in 10 mL 0.1 mM KCl for particle size analysis via dynamic light scattering (DLS).

Once the ideal synthesis conditions were identified, subsequent experiments were performed identically except with the addition of a dialysis step in order to further remove unreacted inorganic constituents and reduce hybrid particle polydispersity. The hybrid particle solution was transferred to laboratory dialysis tubing and placed in a 1 L, 9 mM SDS solution. The dialysis was conducted over three days by replacing the SDS solution daily. The sample was then transferred to a 20 mL vial where the particles were allowed to settle. The heavier composite particles settled faster, leaving the unreacted inorganic constituents suspended in the supernatant. The supernatant was replaced with an equivalent amount of SDS solution and the settled mass resuspended. This process of settling and solvent exchange was carried out two more times to obtain the final hybrid particle suspension.

2.3. Experimental Design

We employed a three-factor Box–Behnken design of experiments to systematically study the role of pH, SDS concentration, and monomer/inorganic weight ratio on the synthesis of composite particles. Each factor was set to two levels (low and high) leading to 8 combinations in the design, with the objective being to control the final particle size of encapsulated microparticles (Table 1). Subsequently, the ideal conditions of pH 4.5, 9 mM SDS, and 4.255 g monomer/g inorganic were chosen for further investigation of encapsulation of alternative inorganic constituents. In addition, the monomer/inorganic weight ratio was systematically varied at these conditions to demonstrate control over the hybrid particle composition.

Table 1. Box–Behnken Experimental Design.

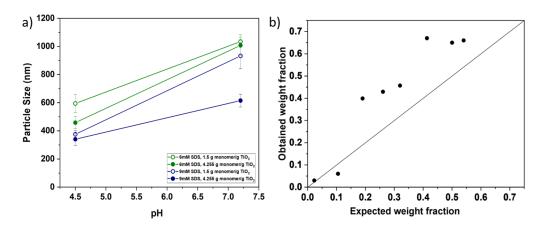| Synthetic Variable	Low Value	High Value
g monomer/g TiO_2	1.5	4.255
pH	4.5	7.2
SDS	6 mM	9 mM

2.4. Particle Characterization

The hybrid particle suspension was diluted (100 μL in 10 mL) in 0.1 mM KCl solution for particle size and zeta potential measurement using dynamic light scattering (Malvern Zetasizer Nano, Malvern, UK). Additionally, inorganic nanoparticles were analyzed (prior to incorporation into the hybrid particles) by DLS for size and zeta potential characterization by suspending them in water at a concentration of 0.1 mg/mL. The reported particle size and zeta potential values were an average of 10 set measurements with 20 sweeps per measurement. Particles were also analyzed by scanning electron microscopy (SEM) by drying a small dilution at room temperature on a silicon wafer before sputter-coating with a thin film of gold. Particle stability was checked using brightfield and fluorescence microscopy (Nikon Ti2-Eclipse inverted microscope, Melville, NY, USA). To quantify the inorganic incorporation, thermogravimetric analysis (TGA, TA instruments Q50, New Castle, DE, USA) was performed after drying a portion of the suspension in a vacuum oven at 60 °C.

3. Results and Discussion

3.1. Hybrid DEMM/TiO_2 Microparticles

We first present results of the design of experiments performed to generate hybrid TiO_2-DEMM microparticles. Particle size measurements were conducted for each experiment that constituted the BBD design. The primary determinant of the particle size was the pH of the reaction, where we found a decreased particle size with lower pH (Figure 1a, Table 2). For the experiments where the surfactant concentration and the monomer to inorganic ratio were at a low level, we measured a particle size of about 520–680 nm for a pH of 4.5 and of about a micron for a pH of 7.2. The particle size decreased at both the pH values in the case wherein the monomer to inorganic ratio was set to a high level while keeping the surfactant concentration at a lower level. We recorded an even further decrease in the particle size in the experiment wherein the surfactant concentration was set to a high level, keeping the monomer to inorganic ratio to the lower limit. Finally, in the case wherein both the factors were set to a high level, we recorded the smallest particle size, ranging from 300–350 nm for a pH of 4.5 and 550–600 nm for a pH of 7.2. It can be inferred from these results that the pH and the surfactant concentration had the most dominant role in influencing the particle size of the resulting composite TiO_2-DEMM microparticles. The individual effects of factors participating in the design influenced the particle size more than the interactive effects of multiple factors.

Figure 1. (**a**) Effect of surfactant concentration, monomer/TiO$_2$ ratio, and pH on DLS particle size of DEMM-TiO$_2$ microparticles. (**b**) Control of TiO$_2$ loading using 9 mM SDS and pH 4.5.

Table 2. DLS results for DEMM-TiO$_2$ hybrid microparticle synthesis.

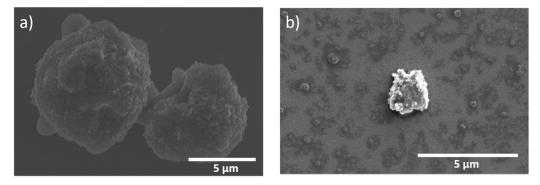| pH	g Monomer/g TiO$_2$	SDS (mM)	Size (nm)
4.5	1.5	6	594 ± 64
4.5	1.5	9	375 ± 27
4.5	4.255	6	458 ± 42
4.5	4.255	9	340 ± 44
7.2	1.5	6	1035 ± 31
7.2	1.5	9	933 ± 92
7.2	4.255	6	1008 ± 75
7.2	4.255	9	615 ± 45

The lower pH corresponds to a higher concentration of H+ ions that are responsible for the chain termination of poly (DEMM). The presence of an acidic environment resulted in polymer chains of lower molecular weight, as reported by Huang et al. [25], and thus resulted in the lower particle size observed in Figure 1a. Additionally, the reduction in particle size at a lower pH is likely due to a difference in polarity between the inorganic surface and the solvent. This minimizes aggregation between the inorganic particles, which leads to smaller composite particles. Control experiments performed without inorganic constituents in identical reaction conditions (pH 4.5, 9 mM SDS) yielded particles with size ranging from 200 to 250 nm. This indicates a lower bound on the particle size and is indirect evidence of the successful incorporation of inorganic nanoparticles, which cause the final particle size to increase.

Our next objective was to quantitatively control the incorporation of the inorganic titania nanoparticles in the organic phase. To investigate that, a range of inorganic concentrations varying from 0.1 wt% per solvent to 5 wt% per solvent were used to synthesize the hybrid microparticles, with a constant pH of 4.5 and 9 mM SDS. An expected weight fraction was determined, indicating the theoretical value of titania present in the polymer matrix. This value illustrates the case wherein all the titania from the reaction is incorporated in the organic phase and assumes complete conversion of the DEMM. The results from TGA were compared to this theoretical value and can be seen in Figure 1b. For increasing titania concentrations in the synthesis reaction, we recorded a higher amount of titania incorporation into the composite particles, as expected. The straight line in Figure 1b represents the scenario where all the titania is incorporated in the polymeric phase, resulting in the expected weight fraction being equivalent to the obtained weight fraction. These calculations were made assuming complete conversion of the DEMM. Since higher weight fractions than expected were measured, this indicates the presence of unreacted monomer or soluble polymer in the synthesis reaction. Using this synthetic approach, we were able to inorganic TiO$_2$ loadings of up to 70% by weight. Based on these results, to

test the applicability of this synthetic procedure to other inorganic constituents, for further study, we chose reaction conditions that resulted in the smallest particle size: pH 4.5, 9 mM SDS 1 wt% inorganic nanoparticles, and 4.255 g monomer/g inorganic.

3.2. Importance of Surface Functionalization for Colloidal Stability

SEM images of the microparticles produced with the optimum synthetic conditions also confirmed the incorporation of the inorganic phase in the organic matrix, as can be seen by the nanoparticles on the surface of the particle under SEM (Figure 2a). However, the particle size measured from SEM image analysis is not consistent with the particle size measurements from light scattering. We obtained a particle size of 5–10 μm from the image analysis as opposed to 350–600 nm from DLS. This inconsistency in particle size is mainly attributed to the tendency of the particles to agglomerate with time and as the solution dries on the SEM stub. The marginal colloidal stability of the emulsion post-synthesis is due to the absence of a stronger surface charge between the hybrid particles. Moreover, the relatively fast sedimentation of the particles encourages agglomerates to form. An immediate solution for overcoming the agglomeration of these hybrid microparticles was to develop a stable colloidal solution by manipulating the charge on the hybrid particle by tuning the chemistry of the ligand stabilizer on the inorganic nanoparticle.
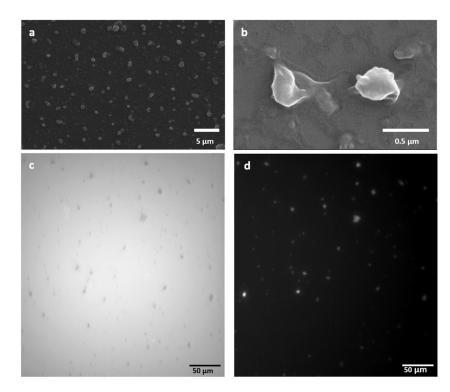

Figure 2. SEM images of particles formed using 9 mM SDS, pH 4.5, and 4.255 g monomer/g TiO$_2$ with either (**a**) bare TiO$_2$ or (**b**) poly-acrylic acid-capped TiO$_2$.

To achieve that, we synthesize hybrid microparticles using TiO$_2$ nanoparticles capped with polyacrylic acid (PA) as the inorganic phase. The PA results in a surface charge of -55 mV on the nanoparticles in comparison to a lower surface charge magnitude (~ -40 mV) in the case of bare titania nanoparticles. A higher magnitude in surface charge resulted in better colloidal stability and lower aggregation of the nanoparticles, and we found this extended to the stability of the hybrid microparticles. The particle size measurements found via DLS and SEM for polyacrylic acid-capped titania hybrid particles (PA-TiO$_2$-DEMM) were in a better congruence in comparison to those with bare titania. DLS revealed minimal change in particle size for the post-dialyzed samples using the two different nanoparticles (257 ± 37 nm for bare TiO$_2$ and 259 ± 10 nm for PA-TiO$_2$); however, the particle size seen under SEM was much smaller for PA-TiO$_2$ (0.7–1.2 μm), as shown in the central particle in Figure 2b.

3.3. Extension to Other Inorganic Constituents

The TiO$_2$ nanoparticles were replaced by the CdTe quantum dots and ZnO nanoparticles, with all other process parameters remaining constant. Post synthesis, we obtained similar precipitation of particles as observed in titania synthesis, and the particles were purified by the same dialysis procedure described above. The CdTe-DEMM composite particles, however, have a lower polydispersity index and formed a homogenous suspension (Figure 3). The surface modification with 3-MPA results in a negative surface charge due to the dissociation of the acidic group, which likely contributes to the improved colloidal stability.
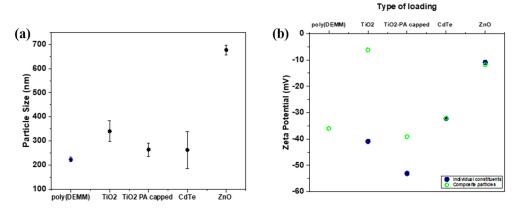
Figure 3. SEM images of CdTe-DEMM hybrid microparticles (**a**,**b**) (300–500 nm), bright-field image (**c**), fluorescence image at 365 nm (**d**), indicating a good colloidal stability and a uniform particle size distribution. (scale bar: (**a**)—5 μm, (**b**)—500 nm, (**c**,**d**)—50 μm).

The incorporation of the CdTe nanoparticles was difficult to validate from the SEM images (Figure 3b). However, CdTe nanoparticles are fluorescent and have an excitation wavelength of 365 nm and an emission wavelength of 700 nm. Fluorescence microscopy was used to investigate whether the CdTe nanoparticles are incorporated in the organic matrix, and as expected, the hybrid microparticles are fluorescent, confirming the presence of CdTe nanoparticles in the composite (Figure 3c,d).

The surface charge of the inorganic constituent appears to dictate the final hybrid particle size, as summarized in Figure 4. The particle size is smaller for inorganic constituents that have a higher magnitude in zeta potential, and SEM imaging of those samples indicated less agglomeration upon drying. Polyacrylic acid-capped titania-DEMM and 3 MPA-capped CdTe-DEMM have a zeta potential of about −40 mV and −30 mV, respectively. These hybrid microparticles have a lower size than hybrid particles with other inorganic constituents. Therefore, a general design principle of incorporating additional inorganic nanoparticles in this synthesis scheme is that a higher inorganic anionic surface charge results in improved colloidal stability, which in turn leads to a lower aggregation and thus a lower particle size.

In addition, zeta potential measurement also revealed the presence of inorganic nanoparticles at the hybrid particle surface, influencing the overall particle charge and contributing to the size stability discussed above. Figure 4b shows the zeta potential of the inorganic nanoparticles suspended in water compared to the final zeta potential of the composite particles. The zeta potential of bare poly (DEMM) microparticles was measured to be about −30 mV. We observe a change in zeta potential post-synthesis that confirms a surface modification of inorganic nanoparticles during synthesis.

Figure 4. (**a**) Particle size of DEMM microparticles without inorganic constituent and with varying inorganic constituents. (**b**) Zeta potential of DEMM microparticles, inorganic nanoparticles, and composite particles with inorganic loading.

An additional result from these measurements is that the zeta potential is reported to significantly decrease for hybrid particles in comparison to their inorganic constituents when the inorganic nanoparticles are TiO_2, but not for CdTe or ZnO. This can be a major factor contributing to their agglomeration, and reinforces the general design principle described above that sufficient inorganic particle surface charge and stability via ligands is necessary to reduce polydispersity and stabilize hybrid microparticles via this technique.

4. Conclusions

A successful system for synthesizing composite inorganic–organic DEMM microparticles has been demonstrated with a variety of inorganic constituents. The composite particle size was predominantly affected by the surfactant concentration and the pH of the reaction solution. The optimal synthetic scheme from the TiO_2-DEMM reaction was applied to other inorganic constituents to evaluate their interaction with methylene malonate to form hybrid particles. Additionally, a correlation between the particle size and its surface charge is presented to emphasize the importance of forming stable colloids of composite particles for reducing coagulation post synthesis. In the future, it will be necessary to test the interaction of these inorganic nanoparticles with standard monomer reactants like styrene (PS) or methyl methacrylate (PMMA) to extend the scope for composite microparticle synthesis. It is also important to further develop strategies for minimizing aggregation to form a stable colloidal suspension of composite microparticles for increasing their applicability as a functional materials. Although the interplay between the nanoscale inorganic and organic constituents is complex, a systematic investigation of their interactions will enrich our understanding in developing composite microparticles with tunable macroscopic properties. The success of using the inorganic constituents reported here indicates the promise of extending these results to additional inorganic nanoparticles and polymers. By incorporating controlled amounts of inorganic nanoparticles, stimuli responsiveness and functionality may be integrated within polymer colloids, which can be leveraged in future studies of their self-assembly into functional metamaterials.

Author Contributions: Conceptualization, J.K. and P.J.B.; methodology, S.J.; investigation, S.J.; visualization, S.J.; writing—original draft preparation, S.J.; writing—review and editing, J.K. and P.J.B.; supervision, J.K. and P.J.B.; funding acquisition, P.J.B. All authors have read and agreed to the published version of the manuscript.

Data Availability Statement: The data presented in this study are available on request from the corresponding author.

Conflicts of Interest: The authors declare no conflicts of interest.

References

1. Glotzer, S.C.; Solomon, M.J. Anisotropy of building blocks and their assembly into complex structures. *Nat. Mater.* **2007**, *6*, 557–562. [CrossRef]
2. Grzelczak, M.; Vermant, J.; Furst, E.M.; Liz-Marzán, L.M. Directed self-assembly of nanoparticles. *ACS Nano* **2010**, *4*, 3591–3605. [CrossRef]
3. Rahman, M.A.; Beltramo, P.J. Rough colloids at fluid interfaces: From fundamental science to applications. *Front. Phys.* **2023**, *11*, 1248706. [CrossRef]
4. Sierra-Martin, B.; Fernandez-Barbero, A. Inorganic/polymer hybrid nanoparticles for sensing applications. *Adv. Colloid Interface Sci.* **2016**, *233*, 25–37. [CrossRef] [PubMed]
5. Qi, D.; Cao, Z.; Ziener, U. Recent advances in the preparation of hybrid nanoparticles in miniemulsions. *Adv. Colloid Interface Sci.* **2014**, *211*, 47–62. [CrossRef]
6. Al Zoubi, W.; Kamil, M.P.; Fatimah, S.; Nisa, N.; Ko, G. Recent advances in hybrid organic-inorganic materials with spatial architecture for state-of-the-art applications. *Prog. Mater. Sci.* **2020**, *112*, 100663. [CrossRef]
7. Kanehira, K.; Banzai, T.; Ogino, C.; Shimizu, N.; Kubota, Y.; Sonezaki, S. Properties of TiO_2-Polyacrylic Acid Dispersions with Potential for Molecular Recognition. *Colloids Surf. B Biointerfaces* **2008**, *64*, 10–15. [CrossRef]
8. Ninomiya, K.; Ogino, C.; Oshima, S.; Sonoke, S.; Kuroda, S.; Sonochemistry, N. Targeted sonodynamic therapy using protein-modified TiO_2 nanoparticles. *Ultrason. Sonochem.* **2012**, *19*, 607–614. [CrossRef] [PubMed]
9. Fredj, D.; Alkarsifi, R.; Pourcin, F.; Liu, X.; Boudjada, N.C.; Pierron, P.; Nourdine, A.; Boujelbene, M.; Fahlman, M.; Videlot-Ackermann, C.; et al. New Antimony-Based Organic-Inorganic Hybrid Material as Electron Extraction Layer for Efficient and Stable Polymer Solar Cells. *ACS Appl. Mater. Interfaces* **2019**, *11*, 44820–44828. [CrossRef] [PubMed]
10. Al Zoubi, W.; Min, J.H.; Ko, Y.G. Hybrid organic-inorganic coatings via electron transfer behaviour. *Sci. Rep.* **2017**, *7*, 7063. [CrossRef]
11. Ramizy, A.; Al-Douri, Y.; Omar, K.; Hass, Z. Optical Insights into Enhancement of Solar Cell Performance Based on Porous Silicon Surfaces. In *Solar Cells-Silicon Wafer-Based Technologies*; InTech: London, UK, 2011. [CrossRef]
12. Raut, H.K.; Ganesh, V.A.; Nair, A.S.; Ramakrishna, S. Anti-reflective coatings: A critical, in-depth review. *Energy Environ. Sci.* **2011**, *4*, 3779–3804. [CrossRef]
13. Schirone, L.; Sotgiu, G.; Califano, F.P. Chemically etched porous silicon as an anti-reflection coating for high efficiency solar cells. *Thin Solid Film.* **1997**, *297*, 296–298. [CrossRef]
14. Moghal, J.; Reid, S.; Hagerty, L.; Gardener, M.; Wakefield, G. Development of single layer nanoparticle anti-reflection coating for polymer substrates. *Thin Solid Film.* **2013**, *534*, 541–545. [CrossRef]
15. Haga, Y.; Watanabe, T.; Yosomiya, R. Encapsulating polymerization of titanium dioxide. *Die Angew. Makromol. Chem.* **1991**, *189*, 23–34. [CrossRef]
16. Xi, J.Q.; Schubert, M.F.; Kim, J.K.; Schubert, E.F.; Chen, M.; Lin, S.Y.; Liu, W.; Smart, J.A. Optical thin-film materials with low refractive index for broadband elimination of Fresnel reflection. *Nat. Photonics* **2007**, *1*, 176–179. [CrossRef]
17. Tan, G.; Lee, J.-H.; Lan, Y.-H.; Wei, M.-K.; Peng, L.-H.; Cheng, I.-C.; Wu, S.-T. Broadband antireflection film with moth-eye-like structure for flexible display applications. *Optica* **2017**, *4*, 678. [CrossRef]
18. Sheth, T.; Seshadri, S.; Prileszky, T.; Helgeson, M.E. Multiple nanoemulsions. *Nat. Rev. Mater.* **2020**, *5*, 214–228. [CrossRef]
19. Sun, J.; Wang, X.; Wu, J.; Jiang, C.; Shen, J.; Cooper, M.A.; Zheng, X.; Liu, Y.; Yang, Z.; Wu, D. Biomimetic Moth-eye Nanofabrication: Enhanced Antireflection with Superior Self-cleaning Characteristic. *Sci. Rep.* **2018**, *8*, 5438. [CrossRef]
20. Jin, L.; Wu, H.; Morbidelli, M. Synthesis of water-based dispersions of polymer/TiO_2 hybrid nanospheres. *Nanomaterials* **2015**, *5*, 1454–1468. [CrossRef]
21. Li, X.; Yu, X.; Han, Y. Polymer thin films for antireflection coatings. *J. Mater. Chem. C Mater.* **2013**, *1*, 2266–2285. [CrossRef]
22. Phillips, B.M.; Jiang, P. Biomimetic Antireflection Surfaces. *Eng. Biomimicry* **2013**, 305–331. [CrossRef]
23. Janssen, R.Q.F. Polymer Encapsulation of Titanium Dioxide: Efficiency, Stability and Compatibility. Ph.D. Thesis, Technische Universiteit Eindhoven, Eindhoven, The Netherlands, 1994. [CrossRef]
24. Roebuck, H.S.; Bon, S.A.F. Cross-Linked Primer Strategy for Pigment Encapsulation. 1. Encapsulation of Calcium Carbonate by Emulsion Polymerization. *Ind. Eng. Chem. Res.* **2019**, *58*, 21130–21141. [CrossRef]
25. Huang, M.; Liu, Y.; Yang, G.; Klier, J.; Schiffman, J.D. Anionic Polymerization of Methylene Malonate for High-Performance Coatings. *ACS Appl. Polym. Mater.* **2019**, *1*, 657–663. [CrossRef] [PubMed]